

3D Reconstruction Using Cubic Bezier Spline Curves and Active Contours (Case Study)

Atefeh Foroozandeh¹, Asghar Kerayechiyan¹, Morteza Gachpazan¹, Mahdi Momennezhad²,
Shahrokh Nasser^{3*}

Abstract

Introduction

3D reconstruction of an object from its 2D cross-sections (slices) has many applications in different fields of sciences such as medical physics and biomedical engineering. In order to perform 3D reconstruction, at first, desired boundaries at each slice are detected and then using a correspondence between points of successive slices surface of desired object is reconstructed.

Materials and Methods

In this study, Gradient Vector Flow (GVF) was used in order to trace the boundaries at each slice. Then, cubic Bezier Spline curves were used to approximate each of obtained contours and to approximate the corresponding points of different contours at successive slices. The reconstructed surface was a bi-cubic Bezier Spline surface which was smooth with G^2 continuity.

Results

Our presented method was tested on SPECT data of JASZCZAK phantom and human's left ventricle. The results confirmed that the presented method was accurate, promising, applicable, and effective.

Conclusion

Using GVF algorithm to trace boundaries at each slice, and cubic Bezier Spline curves to approximate the obtained rough contours yield to the procedure of reconstruction which was fast and also the final surface was smooth with G^2 continuity. So far, some mathematical curves such as spline, cubic spline, and B-spline curves were used to approximate the computed contour during a time consuming procedure. This study presented a 3D reconstruction method based on a combination of GVF algorithm and cubic Bezier Spline curves. There was a good trade-off between speed and accuracy in using cubic Bezier Spline curves which is especially useful for training students.

Keywords: 3D Reconstruction, Cubic Bezier Spline Curve, Gradient Vector Flow (GVF) Field, Left Ventricle, Single Photon Emission Tomography (SPECT) Data

1- Department of Applied Mathematics, School of Mathematical sciences, Ferdowsi University, Mashhad, Iran.

2,3- Department of Medical Physics, Faculty of Medicine, Mashhad University of Medical Sciences, Mashhad, Iran.

2,3- Nuclear medicine Research Center, Imam Reza Hospital, Faculty of Medicine, Mashhad University of Medical Sciences, Mashhad, Iran.

3- Medical Physics Research Center, Faculty of Medicine, Mashhad University of Medical Sciences, Mashhad, Iran.

*Corresponding author: Tel: +98 511 8002328; Fax: +98 511 8002320; Email: NaseriSH@mums.ac.ir

1- Introduction

In many applications in different fields of research such as medical sciences, medical physics, biomedical engineering, and Computer Aided Design (CAD), an object is often known by a sequence of 2D cross-sections (slices) [1, 2]. These slices can be obtained using several imaging techniques such as Computed Tomography (CT), Magnetic Resonance Imaging (MRI), Single Photon Emission Tomography (SPECT), and Positron Emission Tomography (PET). 3D reconstruction surface from given slices is one of the major problems in all mentioned imaging techniques [1]. Till today any attempts have been conducted to address this issue [3-8]. Moreover, several methods have been presented in order to trace boundaries of a given object at each slice. Energy minimizing models such as snakes or active contours have been used extensively for tracing boundaries [3, 4]. In order to address the problems of applying active contour models such as requiring to define a curve extremely near to the true boundary and difficulties in fitting the contour to the concave boundaries, Xu et al. have proposed Gradient Vector Flow (GVF) fields as a new class of external forces [4,8].

Smoothing of the final surface and the speed of 3D reconstruction process are two main factors in almost all 3D reconstruction applications such as students' training. Therefore, in this paper, we present a new fast method for 3D reconstruction which is based on GVF algorithm (in order to trace boundaries at each slice) and cubic Bezier Spline curves (in order to approximate the contours smoothly with G^2 continuity). In the following, some background information including Gradient Vector Flow (GVF) fields and cubic Bezier Spline curves, which are used in this paper, are presented.

1.1. Gradient Vector Flow

Snakes (or active contours) have been presented by Kass et al [3]. Snakes are curves which are defined within an image domain. These curves trace the boundary of the desired

object under the influence of some internal and external forces [4]. Internal forces keep the smoothness of the curve during the deformation. Curves move toward desired boundary of an image under the influence of the external forces [8]. Therefore, snakes have so many applications such as edge detection [3], segmentation [5], and motion tracking [6, 7].

Two types of active contour models are called parametric active contours and geometric active contours [8, 9]. When researchers use parametric active contours they encounter two main problems. First, they need to initialize the snake using a curve extremely near to the true boundary and second they have major difficulties for fitting the final curve to the concave boundaries. In order to address these two issues, Xu et al. presented a new external force called Gradient Vector Flow (GVF) field [4]. In GVF, an external force field $(u(x, y), v(x, y))$ is constructed by diffusing edge force (f_x, f_y) away from the edges to the homogeneous regions and at the same time keeping the constructed field as close as possible to the edge force near the edges [10]. The goal is achieved by minimizing the following energy function:

$$E_{GVF}(u, v) = \frac{1}{2} \iint \mu(u_x^2 + u_y^2 + v_x^2 + v_y^2) + (f_x^2 + f_y^2) \left((u - f_x)^2 + (v - f_y)^2 \right) dx dy \quad (1)$$

Where μ is a non-negative parameter expressing the degree of the smoothness of the field (u, v) . Using variational calculus, Euler equation is obtained as follows [11]:

$$\mu \nabla^2 u - (f_x^2 + f_y^2)(u - f_x) = 0, \quad (2)$$

$$\mu \nabla^2 v - (f_x^2 + f_y^2)(v - f_y) = 0, \quad (3)$$

In order to find the solution of Equations 2 and 3, snake $X(s)$ is made dynamic by considering X as function of time t as well as s , i.e.

$$X(s, t) = [x(s, t), y(s, t)].$$

By solving Equations 2 and 3, GVF field (u, v) is obtained. Finally, snake evolution is given by the following equations [11]:

$$\frac{\partial x}{\partial t} = \alpha \frac{\partial^2 x}{\partial s^2} - \beta \frac{\partial^4 x}{\partial s^4} + u(X, Y) \quad (4)$$

$$\frac{\partial y}{\partial t} = \alpha \frac{\partial^2 y}{\partial s^2} - \beta \frac{\partial^4 y}{\partial s^4} + v(X, Y) \quad (5)$$

1.2. Cubic Bezier Spline Curves

It should be noted that active contour models often produce rough edges [10]. In order to address this issue and obtain smooth edges, computed edges have been approximated using different curves such as cubic Spline [12, 13], cubic B-Spline [14], and NURBS [15]. The computational complexity of above-mentioned curves is very high [12, 14]. In this paper, in order to address this issue cubic Bezier Spline curves are used.

Cubic Bezier Spline curves are presented by G. Farin [16]. A cubic Bezier spline curve is composed of local cubic Bezier curves which are joined smoothly [16, 17]. A cubic Bezier curve ($P(u)$) can be represented via Bernstein polynomial of degree three [17]:

$$B_j^3(u) = \sum_{j=0}^3 \binom{3}{j} (1-u)^j u^{3-j}, \quad u \in [0,1] \quad (6)$$

and the four Bezier points, $p_j (j = 0,1,2,3)$, like below:

$$P(u) = \sum_{j=0}^3 B_j^3(u) p_j = (1-u)^3 p_0 + 3u(1-u)^2 p_1 + 3u^2(1-u) p_2 + u^3 p_3, \quad u \in [0,1] \quad (7)$$

A cubic Bezier spline curve is composed of m local cubic Bezier curves ($P_k(u), k = 0,1, \dots, m-1$). These spline segments can be described by the following equation:

$$P_k(u) = (1-u)^3 p_{3k} + 3u(1-u)^2 p_{3k+1} + 3u^2(1-u) p_{3k+2} + u^3 p_{3k+3}, \quad u \in [0,1], \quad k = 0,1, \dots, m-1 \quad (8)$$

Spline curves pass through each of the end points p_0, p_3, \dots, p_{3m} (called as interpolate points) of the m curve segments. At the points $p_3, p_6, \dots, p_{3m-3}$ (called as Bezier points), two curve segments are joined together [17]. In order to get G^2 continuity at each of the Bezier points, adjoining spline segments must have identical slopes and second derivatives at these points [17]. In other words, the following equations must be satisfied:

$$P'_{k-1}(1) = P'_k(0), \quad P''_{k-1}(1) = P''_k(0), \quad k = 1, \dots, m \quad (9)$$

By using the Equations 8 and 9, we have the following equations:

$$P_{3k} - P_{3k-1} = P_{3k+1} - P_{3k}, \quad k = 1, \dots, m-1 \quad (10)$$

Then, weight points [17] are defined as follows:

$$d_k := P_{3k-1} + \frac{u}{2(1-u)} (P_{3k-1} + P_{3k-2}) = P_{3k+1} - \frac{u}{2(1-u)} (P_{3k+2} + P_{3k+1}), \quad u \in [0,1], \quad \text{for } k = 1,2, \dots, m-1, \quad m \geq 2, \quad (11)$$

Therefore, the following equation is conducted;

$$d_{k+1} := P_{3k+2} + \frac{u}{2(1-u)} (P_{3k+2} + P_{3k+1}), \quad k = 1, \dots, m-1 \quad (12)$$

Using the Equations 10, 11, and 12, three following equations are derived:

$$P_{3k+1} = \left(1 - \frac{u}{2}\right) d_k + \frac{u}{2} d_{k+1}, \quad k = 0,1, \dots, m-1 \quad (13)$$

$$P_{3k+2} = \frac{u}{2} d_k + \left(1 - \frac{u}{2}\right) d_{k+1}, \quad k = 0,1, \dots, m-1, \quad (14)$$

$$P_{3k} = \frac{u}{4} d_{k-1} + \left(1 - \frac{u}{2}\right) d_k + \frac{u}{4} d_{k+1}, \quad k = 0,1, \dots, m-1, \quad (15)$$

In order to solve above equations, the first and the last control points are chosen as follows:

$$P_0 = d_0, \quad P_{3m} = d_m, \quad (16)$$

Therefore, we have

$$P''_0(0) = d_0, \quad P''_{3m}(1) = d_m. \quad (17)$$

Equation 15 is a system of tridiagonal equations in $d_k (k = 0,1, \dots, m-1)$. Forward elimination and backward substitution methods have been used to solve the system of equation 15, with ease. Then the Equations 13 and 14 have been used to calculate other control points P_{3k+1} and P_{3k+2} of every cubic Bezier spline curves. This process is called *control point decision algorithm* for cubic Bezier spline curves [18].

2- Material and Methods

Here, GVF algorithm and cubic Bezier Spline curves were used in order to reconstruct a 3D model of JASZCZAK phantom and actual SPECT data of human's left ventricle. The SPECT datasets from Jaszczak phantom (Figures 1(a), and (b)) were acquired at the Emam Reza hospital of Mashhad, in the

nuclear medicine section, using the SPECT set Siemens, version e.cam, Dual head, parallel Low Energy High Resolution (PLEHR). Main steps of our presented method are as follows:

- Canny edge detector was used to get the edge map of each given slice image.
- Gaussian filter was applied to the image in order to produce an image with flat regions [11].
- The computed GVF algorithm field was used as external force of the snake.
- Initialization of the snake was conducted using a circle which embarrassed the boundary of the image in the largest SPECT slice with the largest image of object.
- Depending on the energy minimization criteria of Xu et al. [4, 8], snake deform (or evolution equation) for the deformation of X, and Y in point (X,Y) was given by the Equations 18 and 19, respectively:

$$X^{t+1}(I_n + \delta A) = X^t + \delta f_x^t$$

$$X^{t+1} = (I_n + \delta A)^{-1}(X^t + \delta f_x^t) \quad (18)$$

$$\frac{Y^{t+1} - Y^t}{\delta} = -AY^{t+1} + f_y^t$$

$$Y^{t+1} = (I_n + \delta A)^{-1}(Y^t + \delta f_y^t) \quad (19)$$

For more information regarding these equations see [4, 8]. The matrix A in the Equations 18 and 19 is a parametric matrix maintaining the parametric continuity. Moreover, f_x and f_y are the gradient vector

force in X and Y directions, respectively. Therefore, snake deformed iteratively to converge on the desired edge [10].

- Cubic Bezier Spline curves were used in order to produce smoothing for detected rough contours [18].
- After approximating of every contour using cubic Bezier Spline curves, these curves were used to interpolate corresponding points in different contours. These spline curves can be understood as the isoparametric curves of bi-cubic Bezier Spline surface in vertical direction [18]. At first, we should match all points in different contours. The number of points in different contours may not be the same, so these points can not be matched directly with each other. Assume that the largest number of points is M. In order to obtain higher accuracy, we could increase the number of some points of other contours to M for other contours points. Here, we do this using the *parameter-based match* method [18].

3- Results

The presented method was tested on SPECT data of JASZCZAK phantom [19] and human's left ventricle. Images of the phantom and human's left ventricle are shown in Figures 1(a) to (c), respectively.

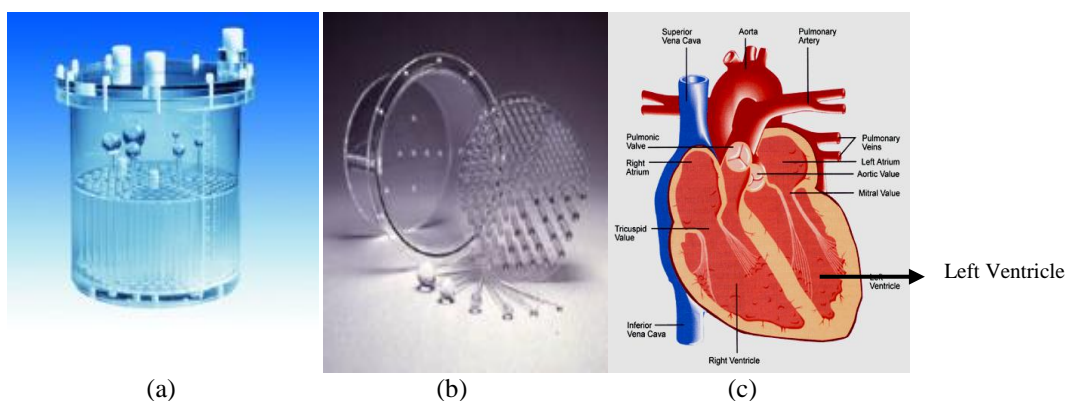


Figure 1. (a) and (b) images of JASZCZAK phantom, and (c) image of human's left ventricle.

One of the advantages of phantom study is that the comparison of obtained result with real data can be conducted with ease. Therefore, in this paper, the method was applied in order to

reconstruct the external surface of the largest sphere in JASZCZAK phantom, as the first experiment. GVF algorithm [20] has several parameters which were determined

empirically. In our first experiment (phantom study), parameters of GVF algorithm were chosen as follows:

$$\alpha=20, \beta=0, \delta=0.6, \mu=10^{-20}, \kappa=1.$$

Where, α : elasticity parameter, β : rigidity parameter, δ : viscosity parameter, μ : regularization parameter of the GVF, and κ is weight of Gradient Vector Flow field. Canny edge detector and Gaussian filtering were used by $\text{thresh}=0.2$, $\text{sigma}=0.3$, $\text{hsize}=1$, and $\text{sigma}=2.5$, as their parameters, respectively.

As mentioned above, first experiment was conducted on SPECT data of the biggest sphere in JASZCZAK phantom. Sixth to the 9th slice of the biggest sphere are shown in Figures 2(a) to (d). In order to increase the speed of the process,

the image of the biggest sphere was extracted from the whole image, as shown in Figure 2(e). Then, its edge map was computed as shown in Figure 2(f). Using Equations 2 and 3, GVF force of the computed obtained edge map was computed. Figures 3(a) to (d) show the computed GVF force and its close up. As shown in Figure 3(e), a circle was considered to initialize the snake. Deformation of the circle was conducted using Equations 4 and 5, as shown in Figures 3(f) to (i).

After tracing boundary at each slice and considering a correspondence between points of successive slices, final surface of the biggest sphere of the phantom was reconstructed as shown in Figure 4.

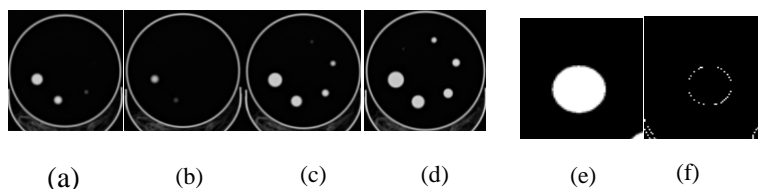


Figure 2. (a) to (d) show 6th slice to 9th slice of phantom, and (e) and (f) are binary image and its edge map, respectively.

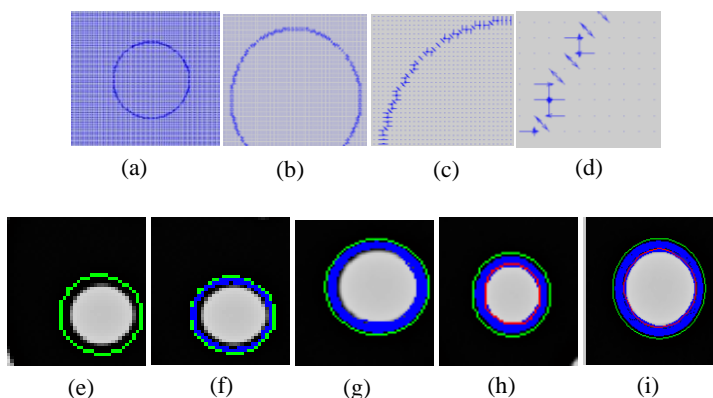


Figure 3. (a) is the computed GVF of showed image, (b) to (d) are the close up of (a), (e) is zoomed view of the initialization of the snake, (f) is the deformation of the snake, (g) is the zoomed of deformation, (h) is the final fit to the boundary which is shown in red color, and (i) is the zoomed view of (h).

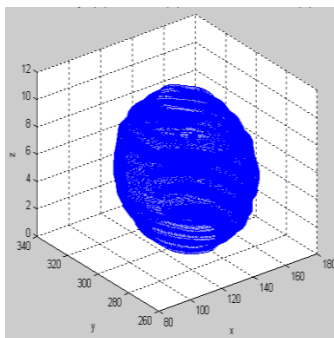


Figure 4. Final reconstructed external surface of the biggest sphere in the JASZCZAK phantom.

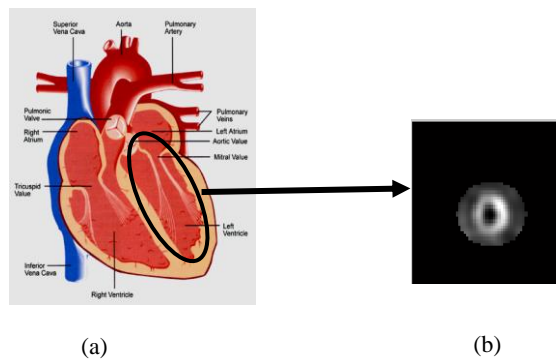


Figure 5. (a) is an image of human's left ventricle, (b) is a 2D cross-section slice of SPECT data of human's left ventricle shown in (a), as an example.

After testing the presented algorithm using the first experiment (phantom study), our method was applied to the actual SPECT data of the human's left ventricle in order to reconstruct its external surface. As an example of 2D cross-section slices of the left ventricle in SPECT data, see Figure 5.

The parameters of GVF algorithm [20] were chosen empirically which were kept constant during the experiment, as follows:

$$\alpha=1, \beta=0, \delta=1, \mu=10^{-20}, \kappa=1$$

Where, α : elasticity parameter, β : rigidity parameter, δ : viscosity parameter, μ : regularization parameter of the GVF, and κ is the weight of GVF field. Canny edge detector was applied with $\text{thresh}=0.001$, $\text{sigma}=0.1$, and Gaussian filtering with $\text{hsize}=1$ and $\text{sigma}=2.5$. Above-mentioned parameters were used in order to reconstruct the external surface of left ventricle. In the following, some of the important steps of this experiment are explained. At first, SPECT slices of left ventricle were binarized, and then edge map of the binary images was computed. As an example of these procedures, see Figures 6(a) and (b), respectively.

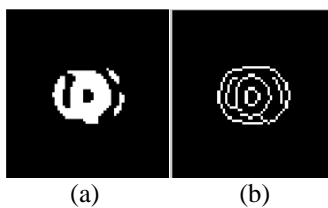


Figure 6. (a) and (b) are the binary image, and the edge map of slice shown in Figure 5(b) shown in (a) and (b), respectively.

GVF field of obtained edge map was computed using Equations 4 and 5. As an example for GVF field of image, see Figure 7(a) and its close up in Figures 7(b) to (d).

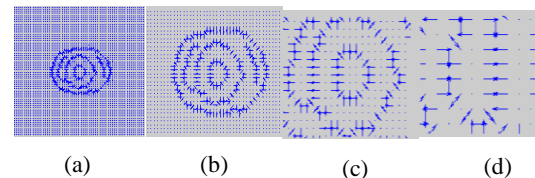


Figure 7. (a) is the computed GVF field and (b) to (d) are the close up of the image shown in (a).

Moreover, as shown in Figure 8(a), the initialization of the snake was done using a circle embraced true boundary of SPECT slice. First, the circle was deformed till fitting to the true external boundary of the image. This procedure is shown in Figures 8(b) to (d). As shown in Figures 9(a) to (c), after tracing boundary at each SPECT slice, using a correspondence between points of successive slices, external surface of the left ventricle was reconstructed, as shown in Figure 9(d).

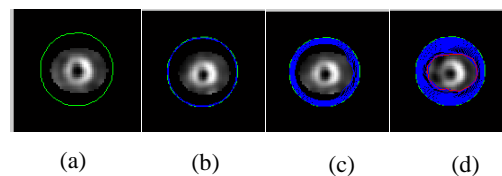


Figure 8. (a) is the initialization of the snake using a circle embraced SPECT slice, (b) and (c) are the deformation of the snake, and (d) is the final fit for the snake which is shown in red color.

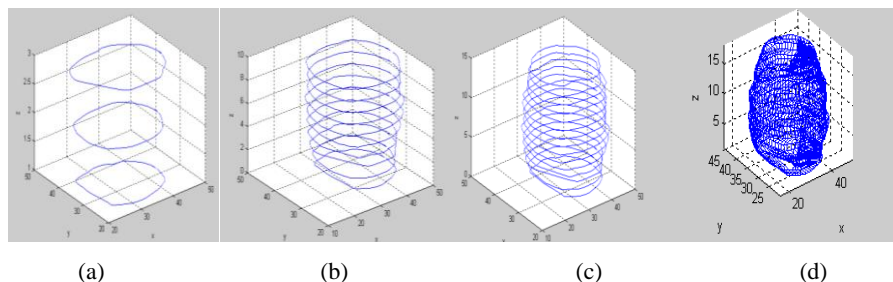


Figure 9. (a) to (c) are some of the traced boundary at successive slices, and (d) is the correspondence between points of successive slices to reconstruct external surface of given left ventricle.

4- Discussion

Three-dimensional reconstruction methods encounter different difficulties which some of them related to the time of reconstruction and the smoothness of the final surface. So far, most of the presented deformable models [8], couldn't address above-mentioned issues. In this paper, tracing boundaries using GVF algorithm and approximating obtained contours by cubic Bezier Spline curves yield to final smooth surface is reconstructed in relatively fast procedure. Based on the results of conducted experiments, there is a good trade-off between speed and accuracy in using GVF algorithm and cubic Bezier Spline curves for approximating the rough obtained edges during a 3D reconstruction method. Using cubic Bezier Spline curves instead of other mathematical curves like cubic spline, and B-spline curves yields a decrease time reconstruction. Moreover, the final surface was smooth with G^2 continuity which is one of the important goals in a 3D reconstruction method.

5- Conclusion

In this paper, a new 3D reconstruction method was presented. At first, one of the best external forces, i.e., GVF force was used in order to trace boundaries at each given 2D cross-section slice. Then, obtained rough edges were

smoothed using cubic Bezier Spline curves. Based on conducted experiments, the presented method has enough capability to be used at each of the related applications especially for students training, surgery planning, etc.

It should be noted that other algorithms such as Charged Contour Model (CCM) [21] and Magnetostatic Active Contour Model (MAC) [22] have been presented in order to trace boundary at each 2D cross-sectional images slice. According to [21] and [22], these methods have high efficiency in SPECT data compared with GVF algorithm. We are going to use these new methods and compare the results with our method in the future to see which is more efficient for 3D reconstruction from actual SPECT data.

Acknowledgements:

This paper was extracted from M.Sc. thesis "Reconstruction from contour lines based on cubic Bezier Spline curves (SPECT images of phantom and human's left ventricle)" presented at Ferdowsi university of Mashhad. The authors would like to thank the office of vice president for research affair at Mashhad University of Medical Sciences, and school of applied mathematics of Ferdowsi University, Mashhad, Iran.

References

1. Park H, Kim K. Smooth surface approximation to serial cross-sections. *Computer-Aided Design*. 1996;28(12):995-1005.
2. Li Z, Ma L, Tan W. Three-dimensional object reconstruction from contour lines. *Proceedings of the 2006 ACM international conference on Virtual reality continuum and its applications*; Hong Kong, China. 1128977: ACM; 2006. p. 319-22.
3. Kass M, Witkin A, Terzopoulos D. Snakes: Active contour models. *Int J Comput Vis*. 1988;1(4):321-31.
4. Chenyang X, Prince JL, editors. Gradient vector flow: a new external force for snakes. *Computer Vision and Pattern Recognition, 1997 Proceedings, 1997 IEEE Computer Society Conference on*; 1997 17-19 Jun 1997.
5. Leymarie F, Levine MD. Tracking deformable objects in the plane using an active contour model. *Pattern Analysis and Machine Intelligence, IEEE Transactions on*. 1993;15(6):617-34.
6. Alwan IA. Object Tracking using Generalized Gradient Vector Flow, *J Eng Technol*. 2011;29(7):1408-24.
7. Wufan C, Shoujun Z, Bin L, editors. LV contour tracking in MRI sequences based on the generalized fuzzy GVF. *Image Processing, 2004 ICIP '04 2004 International Conference on*; 2004 24-27 Oct. 2004.
8. Xu C, Pham DL, Prince JL. Image Segmentation Using Deformable Models. Available at: <http://www.iacl.ece.jhu.edu/pubs/p119b.pdf>. Accessed Oct 10, 2012.
9. Chenyang X, Yezzi A, Jr., Prince JL, editors. On the relationship between parametric and geometric active contours. *Signals, Systems and Computers, 2000 Conference Record of the Thirty-Fourth Asilomar Conference on*; 2000 Oct. 29 2000-Nov. 1 2000.
10. Ghose S. Deformable Model based Computation of Ejection Fraction of Right Ventricle from Cine MRI, A Thesis Submitted for the Degree of M.Sc. Erasmus Mundus in Vision and Robotics, (VIBOT), University of Bourgogne; 2009.
11. Xu C. Deformable models with application to human cerebral cortex reconstruction from magnetic resource images, Ph.D. dissertation, Dept. Electrical Computer Eng., the Johns Hopkins Univ., Baltimore, MD, 1999.
12. Lee WH, Yu K. Bundle block adjustment with 3D natural cubic splines, Ph.D. dissertation, Ohio State University, Geodetic Science and Surveying, 2008.
13. Ben Amour B, Ardabilian M, Chen L. A New 2.5D and 3D Human Face Reconstruction Approach for Recognition. *Journal des Sciences Pour l'Ingénieur*. 2006;7:37-44.
14. Souag N. Three Dimensional Reconstruction of the Left Ventricle using Cubic Uniform B-Spline Curves, 3rd International Conference: Sciences of Electronic Technologies of Information and Telecommunications, Tunisia, March 27-31, 2005.
15. NURBS curves and surfaces tutorial, Available at: <http://docs.happycoders.org/orgadoc/graphics/nurbs/article-en.pdf>. Accessed Oct 10, 2012.
16. Farin GE. *Curves and surfaces for computer-aided geometric design: a practical guide*, Academic Press; 1997.
17. Engeln-Müllges G., Uhlig F., *Numerical Algorithms With C*, Springer; 1996.
18. Li Z, Ma Lz, Tan Wz, Zhao Mx. Reconstruction from contour lines based on bi-cubic Bézier spline surface. *Journal of Zhejiang University Science*. 2006; 1241-6.
19. Flangeless Jaszczak Phantom. Available at: <http://jrtassociates.com/flangelessdeluxejaszczak.aspx>. Accessed Oct 10, 2012.
20. gvf_v5 gvf snake sample program to write matlab Other systems. Available at: http://en.pudn.com/downloads85/sourcecode/others/detail325300_en.html, Accessed Oct 10, 2012.
21. Yang R, Mirmehdi M, Hall DA. Charged contour model for SPECT Cardiac LV Segmentation, Available at: <http://www.cs.bris.ac.uk/Publications/Papers/2000538.pdf>, Accessed Oct 10, 2012.
22. Xianghua X, Mirmehdi M. MAC: Magnetostatic Active Contour Model. *Pattern Analysis and Machine Intelligence, IEEE Transactions on*. 2008;30(4):632-46.